J. Fluid Mech. (1972), *vol.* 56, *part* 3, *pp.* 559–575
Printed in Great Britain

Flow visualization of the near-wall region in a drag-reducing channel flow

By G. L. DONOHUE,† W. G. TIEDERMAN AND M. M. REISCHMAN

School of Mechanical and Aerospace Engineering, Oklahoma State University

(Received 5 June 1972)

The objectives of this study were to determine whether the addition of drag-reducing macromolecules alters the structure of the viscous sublayer and thereby modifies the production of kinetic energy in turbulent wall flows. This was accomplished by visualizing the near-wall region of a fully developed two-dimensional channel flow. Motion pictures were taken of dye injected into the near-wall region. Both water and a dilute drag-reducing polyethylene oxide–FRA solution were used as working fluids. The motion pictures were analysed to determine the spanwise spacing and the bursting rate of low-speed streaks that are characteristic of the viscous sublayer. The amount of drag reduction was established from pressure-drop measurements in pipe flows and a correlation that is independent of hydraulic diameter.

The data show that the time between bursts for an individual streak in a drag-reducing flow has the value for a water flow at the reduced wall shear. However, both the physical and the non-dimensional streak spacing is significantly increased in the drag-reducing flows and thus the spatially averaged bursting rate is decreased. This evidence strongly suggests that the dilute polymer solution decreases the production of turbulent kinetic energy by inhibiting the formation of low-speed streaks. A tentative explanation for this behaviour which is based upon the solution's high resistance to elongational strains and vortex stretching is offered.

1. Introduction

In recent years, numerous experimental studies have shown that the pressure drop for the flow of a Newtonian liquid could be lowered by as much as 80% by the addition of small amounts of certain long-chain molecules. The mechanism by which this reduction in frictional drag occurs has been the subject of much discussion; however, as yet no completely satisfactory explanation has been offered. It is known that drag reduction occurs only when the long-chain molecules are in the near-wall region of the flow and only when the flow of the solvent by itself would have been turbulent. It is also well known that the dilute polymer solution has essentially the same density and the same viscosity in simple

† Present address: Naval Undersea Research and Development Center, Pasadena, California.

shear as the solvent. The only significantly different physical property of these dilute polymer solutions is their ability to form filaments. This characteristic has been attributed to the solution's high resistance to axisymmetric strains (see Lumley 1969). Even so there has been no clear experimental evidence that this unusual property of the solution is the mechanism by which drag reduction occurs. Hence the primary purpose of the flow visualization experiments reported here was to gain a further understanding of how the dilute polymer solution interacts with and changes the turbulent flow structure in the near-wall region.

These experiments were motivated by the observations of Wells & Spangler (1967) and the experiments of Kim, Kline & Reynolds (1971). Wells & Spangler conclusively demonstrated that drag reduction is a wall phenomenon. When they injected a polymer solution at the centre-line of a pipe, drag reduction did not begin until the polymer diffused into the wall region. However, when the polymer solution was injected through a slot directly into the wall region, drag reduction began immediately. Numerous experiments by various investigators have shown that the dominant feature of this near-wall region of a turbulent flow is a streaky structure which is caused by a spanwise variation in the axial velocity component. The low-speed streaks of this structure periodically lift away from the wall into the buffer region, where they oscillate and then burst violently away from the wall region. Kim *et al.* showed that 70 % of the turbulent kinetic energy is produced during these bursts.

The conclusion which is suggested by these two studies is that in some way the drag-reducing solution reduces the amount of bursting and hence the production of turbulence is decreased. Since the flow is fully developed the decrease in production leads directly to a decrease in dissipation and lower friction factors.

The experiment of Wells & Spangler (1967) is crucial to this reasoning because Corino & Brodkey (1969), Clark & Markland (1971), Kim *et al.* (1971) and Wallace, Eckelmann & Brodkey (1972) have all presented evidence which shows that the complete cycle of turbulence production includes large-scale inrushes or sweeps as well as the outward bursting. The production cycle, as described by Corino & Brodkey, includes a local deceleration of the fluid in the near-wall region, ejection of slow fluid outwards from the wall and finally a sweep of higher velocity fluid moving towards the wall (some sweeps move nearly parallel to the wall but they yield little positive production). Consequently, the demonstration that the polymer must be in the wall region means that it is most likely that the direct effect of the solution is upon the streaky structure and its bursting.

Gadd (1965) was perhaps the first person to suggest that the drag-reduction phenomenon is related to the streaky structure and a reduction in its bursting rate. However, reductions in bursting had been previously noted in non-drag-reducing flows. Kline *et al.* (1967) and Moretti & Kays (1965) showed that acceleration decreased the bursting rate, increased the streak spacing and caused the heat transfer to assume 'laminar-like' values. Halleen & Johnston (1967) showed that Coriolis forces would also reduce the bursting rate of low-speed streaks. Even more significantly, they showed that as the bursting rate decreased so did the wall shear.

The only studies which have specifically investigated the wall-region structure of a drag-reducing flow are the recent investigations of Fortuna & Hanratty (1972) and Eckelman, Fortuna & Hanratty (1972). In both studies electrochemical techniques were used to show that the average non-dimensional spanwise spacing λ^+ of the sublayer's streaky structure is larger in dilute polymer flows than it is in water. Moreover, both reported that λ^+ increases as the amount of drag reduction increases.

This study's experimental objective was to quantify visually the effect of polyethylene oxide–FRA† on the sublayer of a fully developed two-dimensional channel flow. Both bursting rates and spanwise spacings of the low-speed (low momentum) streaks were measured in flows of water and 139 parts per million by weight (w.p.p.m.) polymer solutions. The streaks were made visible by dye which was carefully seeped into the sublayer through wall slots. Motion pictures were made of the flow and consequently some subjective comparisons can also be made between the drag-reducing flows and flows of water. The experimental conditions covered a range of drag reductions from 0 to 52%. The wall shear velocities varied from 0·0043 to 0·0155 m/s as the Reynolds number based on mass average velocity and hydraulic diameter varied from 6000 to 22800.

The results support the conclusion that the dilute polymer solution decreases the production of turbulent kinetic energy by inhibiting the formation of low-speed streaks. A tentative explanation for this behaviour is based upon the solution's high resistance to elongational strains. The study also shows that the time and length scales needed to characterize the drag-reduction phenomenon are those of the near-wall region.

2. Experimental methods

2.1. *Flow facility*

The experiments were conducted in the plastic and stainless-steel apparatus shown in figure 1. The channel walls are single pieces of 12·7 mm Plexiglas. The channel is 40·4 mm wide, 451 mm tall and 2·54 m long. The dye slots used to visualize the near-wall region are 0·127 mm wide and 178 mm long and are located 44 and 51 channel widths downstream from the two-dimensional bell-mouth entrance. There are no pumps in the flow loop and hence mechanical degradation of the drag-reducing additive is minimal. Fluid is forced through the channel by pressurizing the 2·27 m^3 upstream tank. The fluid is caught and contained during the run in an open-top 2·27 m^3 tank downstream of the channel. If the solution is to be reused, it can later be returned to the upstream tank by gravity. A weir downstream of the channel exit is used to measure the flow rate and to maintain a constant downstream head.

2.2. *Flow visualization*

The dye injection, burst counting and the streak spacing measurements were esssentially the same as those described by Kline *et al.* (1967). The most critical elements of the dye-injection technique are the dye slot and the injection rate of

† Molecular weight $7{\cdot}5 \times 10^6$.

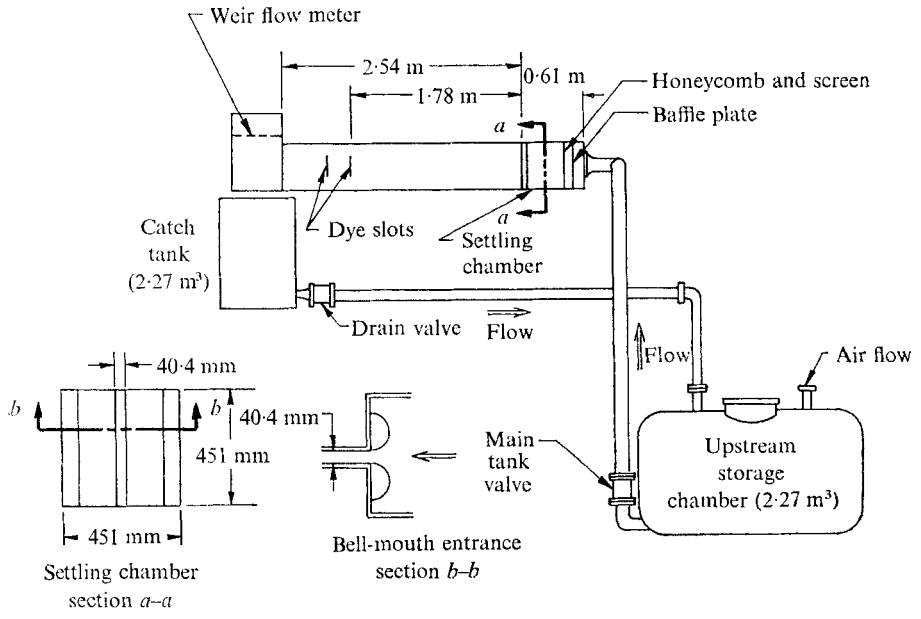

FIGURE 1. Flow system.

the dye. In this case, the two 0·127 mm dye slots were milled normal to the wall and normal to the streamwise direction with a slitting saw. By careful machining the slots were made free of burrs and since there were no joints in the channel walls, wall disturbances were minimized. The flow rate of the dye was also carefully controlled so that the dye caused a minimal disturbance to the wall regions. This was illustrated by experiments in the laminar and transition flow regimes. In a laminar flow, the dye (an 8 % solution of blue food colouring) left the slot in a uniform sheet which travelled downstream as close to the wall as one could determine. In transitional flows, the uniform sheet was randomly disturbed by turbulent spots moving downstream. Inside these spots the characteristic streaky structure of a turbulent wall region existed. On the basis of these experiments, similar experiments by Runstadler, Kline & Reynolds (1963) and the fact that the dye flow rate was always less than 10 % of the sublayer flow rate, it is believed that the dye only made visible, and did not cause, the flow phenomena which were observed. This conclusion is strengthened by the fact that the results in water flows agree with streak spacing and bursting measurements made with hydrogen bubbles (Kline *et al.* 1967; Kim *et al.* 1971), hot-wire probes (Gupta, Laufer & Kaplan 1971) and flush-mounted electro-chemical probes (Fortuna & Hanratty 1972).

The upstream dye slot was used for measuring the bursting rates of the streaks. Since a side view was necessary to identify the bursts of dye leaving the wall region, the slot was masked to a 17·0 mm span so that only one or two streaks would be marked at any one time. In this way, the bursting streaks did not obscure each other and accurate counts could be made. The bursting rate films had a field of view which included the slot and a 203 mm region downstream. These films were separately timed to within $\pm$ 0·6 s with an electric timer.

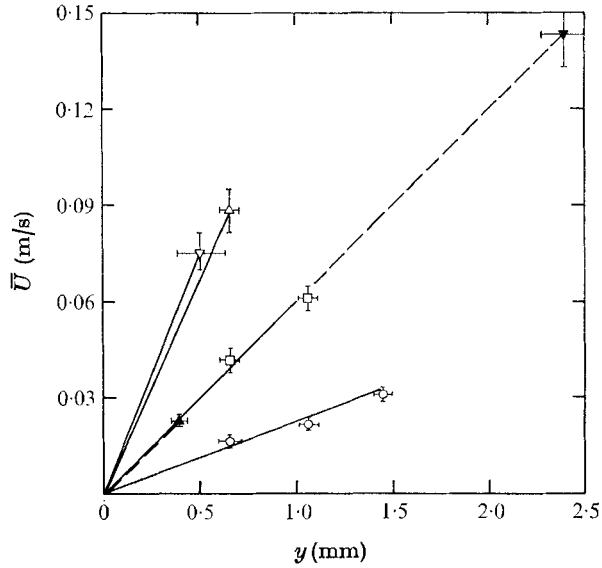

FIGURE 2. Mean velocity profiles in the near-wall region. ○, Re = 6000, solvent; □, Re = 11000, solvent; ▽, Re = 15000, solvent; △, Re = 18000, solvent; ▼, Re = 15000, polymer; ▲, Re = 18000, polymer.

The unmasked dye slot was used for measuring streak spacing. These measurements were made by randomly stopping the film and counting the number of streaks visible in a 102 mm span. The streaks were counted along a line which is parallel to and from 38 to 77 mm downstream of the dye slot. An average streak spacing was calculated for each flow condition from a number of randomly selected frames. The films were spatially calibrated with a grid which had 2·54 mm divisions.

2.3. *Wall shear in water*

The wall shear and the wall-shear velocities used throughout this study are based upon measurement of the velocity in the viscous sublayer, where the average velocity varies linearly with the distance normal to the wall. These measurements were made with a laser anemometer measuring individual realizations (LAMIR). As was previously reported by Donohue, McLaughlin & Tiederman (1972) the laser system was used to show that the water flow in the channel are standard two-dimensional turbulent channel flows. Here only the measurements of the mean streamwise velocity $\bar{U}$ in the viscous sublayer are used and these are shown in figure 2. From these linear plots the wall shear τ_0 is determined from

$$\tau_0 = \mu(\partial\bar{U}/\partial y)_{y=0}. \tag{1}$$

Table 1 shows these same data in wall-layer co-ordinates U^+ and y^+. The bulk of the measurements were made at y^+ values which are normally considered to be inside the viscous sublayer. U^+ is $\bar{U}/v^*$ and y^+ is yv^*/ν, where v^* is the wall-shear velocity $(\tau_0/\rho)^{\frac{1}{2}}$, ν is the kinematic viscosity and ρ is the density of the fluid. The measurement made in the dilute polymer solution at $y^+ = 15$ is an

Re	$\bar{U}_{av}$ (m/s)	Run type	$\nu \times 10^6$ (m²/s)	y (mm)	$\bar{U}$ (m/s)	v^* (from figure 3) (m/s)	y^+	U^+
6000	0·0701	Solvent	0·89	0·66	0·017	0·0042	3·1	4·0
				1·07	0·022		5·0	5·2
				1·45	0·031		6·8	7·4
11000	0·131	Solvent	0·89	0·66	0·042	0·0073	5·4	5·7
				1·07	0·061		8·8	8·4
15000	0·207	Solvent	1·02	0·51	0·075	0·0112	6·7	5·6
18000	0·210	Solvent	0·89	0·66	0·088	0·0111	8·2	7·9
15000	0·207	Polymer	1·43	2·39	0·143	—	15·2	15·6
18000	0·210	Polymer	1·36	0·38	0·022	—	2·5	2·5

TABLE 1. Summary of near-wall velocity measurements

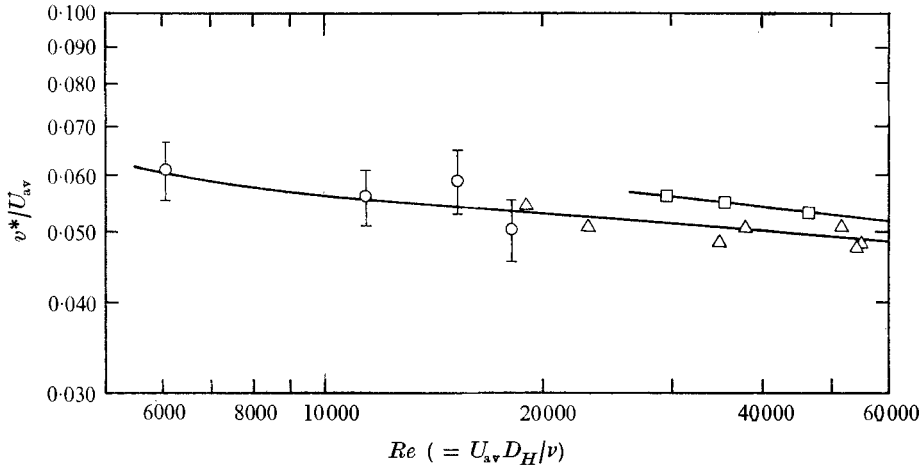

FIGURE 3. Non-dimensional wall-shear velocity for two-dimensional channel flows. ○, present study; △, Clark (1968); □, Hussain & Reynolds (1970).

exception. However, the best velocity measurements in a dilute polymer flow (see Rudd 1972) indicate that a $y^+ = 15$ is just at the outer edge of a thickened viscous sublayer for a drag-reducing flow.

In most cases, the flow visualization experiments and the velocity measurements were made neither at the same time nor in precisely the same conditions. However, the data reduction required knowledge of the wall-shear velocity during the flow visualization runs. These wall-shear velocities were determined using figure 3, which shows the Reynolds number dependence of the wall-shear velocity normalized by the mass-average velocity. Since the Reynolds number is based upon the mass-average velocity and the channel's hydraulic diameter of 74·4 mm, the wall-shear velocity for all water flow can be determined from figure 3 and a measurement of the mass-average velocity.

Figure 3 also shows the data of Clark (1968) and Hussain & Reynolds (1970). Clark's data, which are also based upon the slope of the velocity profile at the wall,

is in good agreement with the present study. Hussain's data, which are based upon pressure-drop measurements, yield higher wall-shear values because these measurements include the corner and endwall losses. It should be pointed out that it is more appropriate to use a wall-shear velocity computed from the velocity gradient in the sublayer for characterizing turbulent wall structure than a wall-shear velocity found from a 'law of the wall' fit (as demonstrated by Kline *et al.* 1967) or a friction factor correlation (which averages channel corner effects into the computed local wall shear).

2.4. *Wall shear in the dilute polymer solutions*

While it was possible to measure the velocity profile in the dilute polymer solution directly using the laser anemometer, it is not easy to do this at the same time as motion pictures are being made. The difficulty is due to the relatively short run time with the blow-down system, the relatively slow data acquisition rate with the laser anemometer measuring individual realizations, and degradation of the solution in the free fall after the weir. Consequently, in most cases the wall shear for the dilute polymer flows was determined from a measurement of the flow rate, the correlation shown in figure 3 and the drag-reduction correlations shown in figures 4(*a*), (*b*) and (*c*).

The percentage drag reduction is defined to be

$$100 \times [1 - \tau_0/(\tau_0)_s]. \tag{2}$$

$(\tau_0)_s$ is the wall shear for a given flow rate of water and τ_0 is the wall shear for the dilute polymer solution flowing at the same rate in the same channel. The correlations shown in figure 4 were established for each batch of dilute polymer solution by measuring the pressure drop in two 2·75 m long stainless-steel tubes, 10·8 mm and 21·2 mm in diameter, at several flow rates for both water and the drag-reducing solution. Such a correlation has been shown to be valid by Whitsitt, Harrington & Crawford (1969) for pipes ranging in diameter from 4·57 to 152 mm. The correlations were also verified in this study by measuring the wall shear in two dilute polymer channel flows.

In these two cases the wall shear in the dilute polymer flows was estimated by measuring the velocity gradient at the wall with the laser anemometer, by measuring the viscosity of the dilute polymer solution with a Brookfield viscometer and by using equation (1). This technique is valid when the solution is thermodynamically dilute and the viscosity is independent of shear rate (see Merrill *et al.* 1966). A thermodynamically dilute solution is one in which the spherical packing of the polymer molecules based on the estimated root-mean-square coil diameter is less than 74 %. For the polyethylene oxide–FRA molecules used here the solutions are thermodynamically dilute for concentrations less than about 240 w.p.p.m.

Throughout this study a 139 w.p.p.m. solution of polyethylene oxide–FRA was used as the drag-reducing fluid. This solution was chosen because the large hydraulic diameter of the channel required the most effective additive and because this particular solution is thermodynamically dilute. As a check, the viscosity of a 100 w.p.p.m. solution of polyethylene oxide–FRA was measured

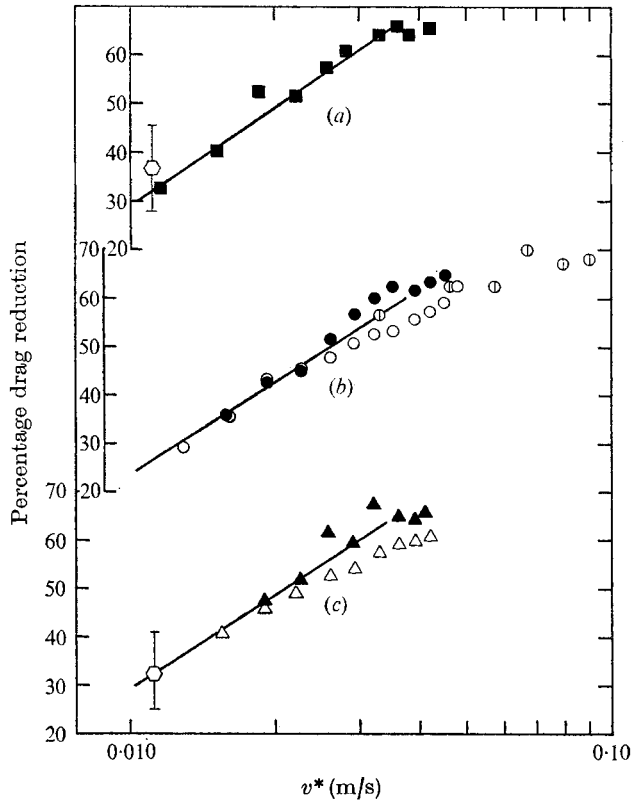

FIGURE 4. Drag-reduction correlations for 139 w.p.p.m. solution of polyethylene oxide–FRA. (*a*) Solution *A*, LAMIR; (*b*) solution *B*, visual; (*c*) solution *C*, LAMIR and visual. ■, ●, ▲, 21·2 mm pipe data taken before the channel run; ○, △, 21·2 mm pipe data taken after the channel run; ⦶, 10·8 mm pipe data taken after the channel run; ⬡, LAMIR velocity gradient data.

with a Brookfield viscometer over a range of shear rates from 14·7 to 73·4 s^{-1}.† The viscosity was constant, which indicates that the solution is effectively Newtonian in simple shear.

Despite the fact that the utmost care was used in mixing the drag-reducing solutions there were still differences between each batch. Thus a friction reduction correlation was established for each batch as shown in figure 4. Each solution was also checked for degradation by making pressure-drop measurements in the pipes before and after the channel runs.

3. Results

A summary of the flow conditions and the quantitative results of this study are shown in table 2. In addition, subjective comparisons can be made from the motion pictures, which show that the polymers produce a marked change in

† The wall-shear rates varied from 36 to 169 s^{-1} in the dilute polymer flow visualization experiments.

U_{av} (m/s)	Polymer concentration (w.p.p.m.)	Percentage drag reduction	v^* (m/s)	$\nu \times 10^6$ (m^2/s)	F (burst/s m)	λ (mm)	λ^+	$\bar{T}_B = 1/F\lambda$ (s/burst)
0·0701	0	0	0·0043	0·89	7·5	19·6	94	6·9
0·131	0	0	0·0073	0·89	28·0	12·7	104	2·8
0·210	0	0	0·0113	0·89	107	7·6	96	1·2
0·207	0	0	0·0113	1·02	134	9·5	105	0·79
0·131	139	16	0·0067	1·25	14·2	23·1	124	3·1
0·131	139	16	0·0067	1·25	17·3	—	—	2·5†
0·210	139	28	0·0095	1·25	—	17·0	128	—
0·210	139	28	0·0095	1·25	33·9	—	—	1·7†
0·207	139	33	0·0092	1·43	26·8	27·2	174	1·4
0·439	139	52	0·0156	1·43	—	17·0	185	—

† Used λ from previous run at same flow conditions to compute $\bar{T}_B$.

TABLE 2. Summary of flow conditions and major results

the structure of the near-wall region for turbulent flows of equal flow rates. The two most obvious changes noted when viewing the films are (i) a decrease in the quantity and the intensity of the spatially averaged bursting rate of the low-speed streaks; (ii) a decrease in variations of the spanwise velocity profile (i.e. the spanwise velocity profile is 'smoothed' and there seems to be a decreased tendency for low-speed streak formation). A 16 mm colour film has been prepared and is available for viewing (Donohue & Tiederman 1971); it illustrates these qualitative changes in the turbulent structure.

Figure 5 shows the low-speed-streak bursting rates in both water and dilute polymer solutions. F is the bursting rate per metre of dye slot. The dotted line is the zero-pressure gradient correlation for turbulent boundary layers established by Kline *et al.* (1967). The solid line was obtained by applying a pressure-gradient correction to the Stanford data. The water data agree quite well with previous measurements and the drag-reducing data show significantly reduced spatially averaged bursting rates. The amount and character of this reduction can best be illustrated by a numerical example. When the water flow and the 33 % drag-reduction flow (solution C) with mass-average velocities of 0·207 m/s are compared, it is apparent that F for the drag-reducing flow is considerably lower than F for a water flow with the wall shear of the drag-reducing flow. Specifically, a decrease in v^* from 0·0113 m s to 0·0092 m s for a water flow corresponds to a decrease in F from 134 bursts/s m to 74·7 bursts/s m. However, the drag-reducing flow with $v^* = 0{\cdot}0092$ m/s has a spatially averaged bursting rate of 26·8. Further reference to this point will be made in the discussion (§ 4). In this figure, as in all others, brackets on the data points indicate the 95 % confidence intervals.

It should be noted that Donohue (1972) was uncertain as to whether or not even more drastic reductions in the bursting rates were sometimes occurring. To resolve this question, a new polymer batch was prepared (labelled solution C) and was filmed for $2\frac{1}{2}$ times the previous time-averaging period to obtain a better

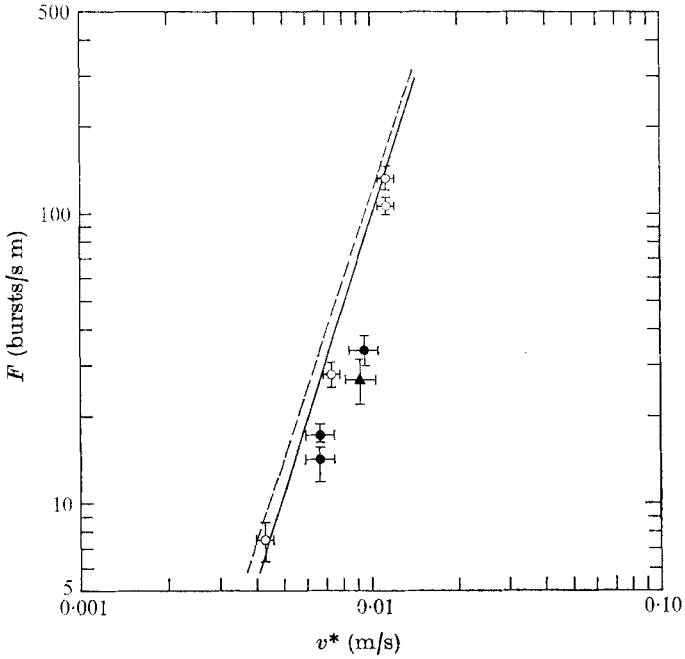

FIGURE 5. Spatially averaged bursting rates in water and dilute polymer solutions. ○, water; ●, solution B; ▲, solution C; – – –, zero pressure gradient, Kline *et al.* (1967); ——, corrected for pressure gradient.

statistical measure of the bursting rates in a freshly prepared solution. In addition, a simultaneous *in situ* velocity-gradient estimate was made to remove any ambiguity that might have been present in the indirect measurement of wall shear described earlier. The percentage drag reduction measured by both the pipe pressure drops and the wall shear determined from laser anemometer measurements are shown in figure 4(*c*). The simultaneously measured bursting rate shown in figure 5 supports the majority of the data obtained in solution B and indicated that the abnormally low bursting rate previously reported was in error owing to an insufficient time-averaging period. This simultaneous estimate of the wall shear with the laser anemometer also supports the data obtained in solution A and indicates that the pipe pressure-drop measurements provide an accurate measure of the drag-reduced wall shear in the channel.

The streak-spacing data are shown in figure 6, where it is seen that the average non-dimensional spacing $\lambda^+ = \lambda v^*/\nu$ of the streaks is greater in the drag-reducing solution than it is in water. Here λ is the average spanwise streak spacing. The solid and dotted lines in figure 6 are from the measurements of Halleen & Johnston (1967) and the agreement between the two water experiments is obviously quite good.

The data in figure 6 represent streak-spacing measurements in two different 139 w.p.p.m. batches of polyethylene oxide (solutions B and C). In general any two polymer solutions of equal concentration will not produce exactly the same amount of drag reduction at a given wall shear (see figures 4(*a*), (*b*) and (*c*)). It is

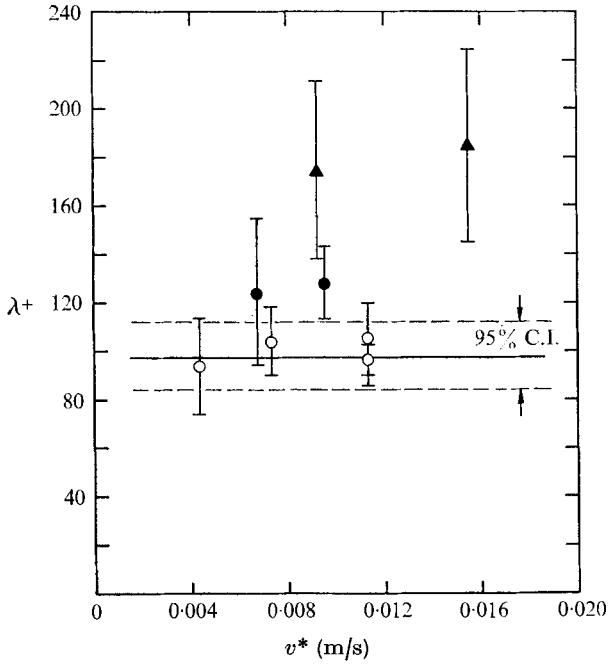

FIGURE 6. Non-dimensional streak spacings in water and dilute polymer solutions. ○, water; ●, solution *B*; ▲, solution *C*; ——, Halleen & Johnston (1967).

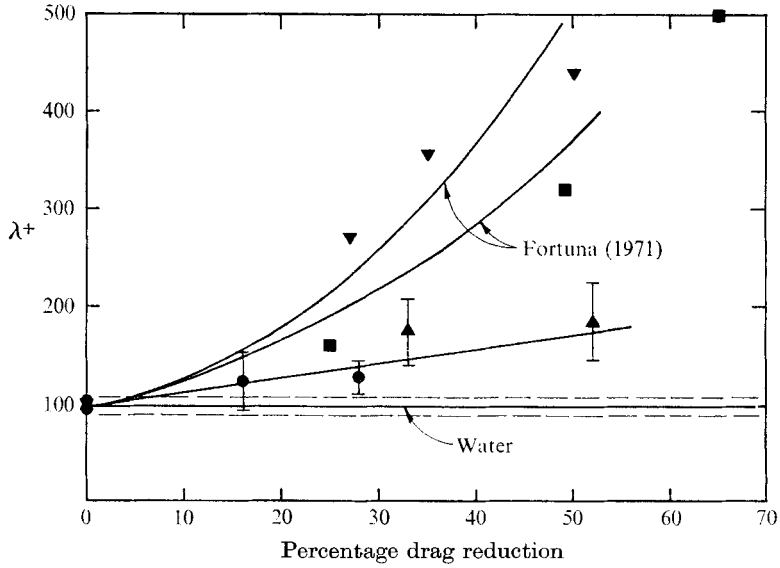

FIGURE 7. The effect of the percentage drag reduction upon the non-dimensional streak spacing. ■, Eckelmann *et al.* (1972); ▼, Fortuna & Hanratty (1972). Present study: ●, solution *B*; ▲, solution *C*.

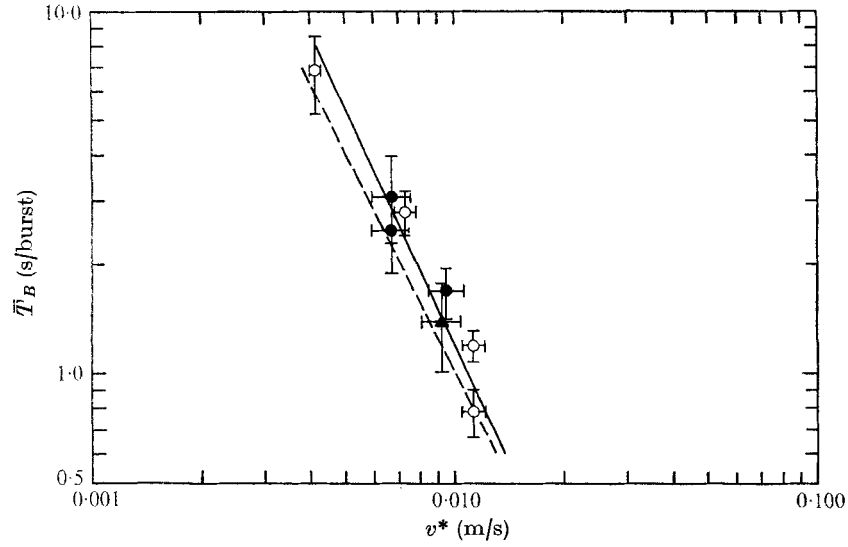

FIGURE 8. The average time between bursts for water and dilute polymer solutions. ○, water; ●, solution B; ▲, solution C; – – –, zero pressure gradient, Kim *et al.* (1971); ——, corrected for pressure gradient.

for this reason that pressure-drop measurements are made for each solution. Figure 7 shows that λ^+ is an increasing function of the percentage drag reduction. Figure 7 also shows the data of Fortuna & Hanratty (1972) and the data of Eckelman *et al.* (1972) as well as the functional dependence of λ^+ predicted by the sublayer models of Fortuna (1971). Our data are in qualitative agreement with these previous measurements but in general show a much smaller increase in λ^+. The discrepancy with Fortuna's data may be due to the fact that Fortuna used a different polymer–solvent combination or it may be caused by too long an averaging time in Fortuna's cross-correlations. The results of Gupta *et al.* (1971) show that it is very easy for time-averaged spanwise cross-correlations to 'smear out' the positive correlations produced by the presence of the adjacent low-speed streaks. Only by carefully taking small time-averaging periods did Gupta find the positive correlations associated with the low-speed regions. The discrepancy with the data of Eckelman *et al.* (1972) may be the result of their data reduction, in which some zero crossings were ignored. In this study, all streaks were used in calculating an average λ. In any case, all the data show that the non-dimensional streak spacing increases with increasing drag reduction. It should be pointed out that all of the drag-reducing visual data shown have been correlated by using the reduced wall shear. The structural differences between water and a dilute polymer solution are even more dramatic if the flows are compared at a constant flow rate.

Figure 8 shows how the time $\bar{T}_B$ between bursts is affected by the polymer: $\bar{T}_B = 1/F\lambda$. Here it seems that the average time between the bursts of an individual streak in the drag-reducing solutions is at the level expected for a water flow at the reduced wall shear. Again the dotted and solid lines show the Stanford correlation

and the pressure-gradient corrected correlation. The use of v^* to correlate the data in figure 8 is not intended to imply that the time between bursts should scale on inner variables. In fact, Laufer & Badri Narayanan (1971) and Rao, Narasimha & Badri Narayanan (1971) have shown that for very large ranges of the momentum-thickness Reynolds number the time between bursts in a turbulent boundary layer correlates with the outer variables of either boundary-layer thickness or displacement thickness and free-stream velocity. Here, since the range of Reynolds number is small and since complete velocity profiles were not measured in the dilute polymer flows it was decided to use the inner variable scaling reported by Kline *et al.* (1967). Much larger variations in Reynolds number must be studied to test critically the scaling for dilute polymer flows.

4. Discussion

The most obvious feature about the results is that the near-wall flow structure does change when drag reduction occurs. The spatially averaged bursting rate of low momentum streaks is lower than the bursting rate of a Newtonian flow at the reduced wall shear and the streak spacing is larger. Thus the drag-reducing flow is not simply a standard turbulent flow at a reduced wall shear. Instead the drag-reducing flow has a different near-wall flow structure and apparently a different or at least a modified turbulent production process.

The best evidence now suggests that turbulence production in a non-drag-reducing flow occurs through a sequence of events whose important aspects are: formation, lift-up, oscillatory growth and 'breakup' of the low-speed streaks followed by a larger scale inrush or sweep. In a fully developed flow such as the one studied, all these processes are in statistical balance and equilibrium. To affect turbulence production it is only necessary for the polymer additive to break this sequence by affecting one of the processes. Once this has occurred the remainder of the sequence will adjust and a new equilibrium condition will exist. Consequently caution should be used in discussing how the polymer affects production. However, some possibilities appear considerably more likely than others and these will be suggested as the mechanism by which drag reduction occurs.

It should be emphasized that it is clear that the polymer additive does reduce the production of turbulence and that this effect occurs in the near-wall region. The suppression of the spatially averaged bursting rates (50–70 % of the net production occurs during bursting according to Kim *et al.* (1971) and Wallace *et al.* (1972)) and the fact that the polymer must be in the near-wall region are the primary experimental support for this conclusion.

It is also clear that drag reduction does not occur through the interaction of a fluid eddy with an individual polymer molecule. This is demonstrated by the data of Paterson & Abernathy (1970), which indicate that drag reduction exists in the limit of infinite dilution. It is also suggested by the large disparity in size which exists between the smallest scales of fluid motion and the largest dimension of the polymer molecule. Instead the mechanism of drag reduction is most likely associated with a continuum property of the solution.

Fortunately, the most dramatic rheological difference between a dilute

polymer solution and a Newtonian solvent provides a reasonable explanation of how turbulence production is altered in the near-wall region. Physically the difference exists because the polymer solution has a higher resistance to axisymmetric strains than it does to rotational strains. This high resistance to axisymmetric strains accounts for the filament-forming tendencies of dilute polymer solutions as well as the 'stringy' appearance which occurs when a solution is draining from an object. This resistance to axisymmetric strains may be quite high. For example, Lumley (1969) estimated that the viscosity of a 50 w.p.p.m. solution of polyethylene oxide (molecular weight of 6×10^4) in axisymmetric strain is four orders of magnitude larger than the viscosity in rotational strain. Since axisymmetric strains are believed to be prevalent in both the formation of the streaky structure and the bursting of low momentum streaks, an explanation of the drag-reduction mechanism based upon this property is consistent with both the fluid motions and the capabilities of the dilute polymer solution.

Vortex stretching during streak formation is discussed by Kline *et al.* (1967) in their description of the physical structure of non-drag-reducing turbulent wall flows. They suggest that the stretching and compressing of *spanwise* vortex elements in the region very near the wall lead to locally high- and low-speed zones in the spanwise direction. The zones of vortex compression are the low-speed regions where the dye collects and the streaks form. The intermittent and random formation of these zones produces intense local shear layers which eventually give rise to the burst of the streak away from the wall.

As described by Kim *et al.* (1971), vortex stretching may also occur during the second phase of the bursting process. The entire bursting process is observed to go through three distinct phases:

(i) Low-speed streak formation and lift-up into the buffer region, at which time an instantaneous inflexional velocity profile is observed.

(ii) Rapid growth of an oscillatory motion that occurs in one of three distinct modes downstream of the inflexional zone.

(iii) Streak 'breakup' in a chaotic fluctuation.

The most common mode of oscillatory motion is the rapid growth and stretching of a *streamwise* vortex. This is observed in two-thirds or more of the cases in non-drag-reducing flows. The two less common modes of oscillatory growth are a repeated oscillation termed a 'wavy motion' and the relatively rare occurrence of a secondary spanwise vortex.

Thus vortex stretching can occur both during the formation of the streaky structure and during the rapid growth of the oscillatory motion. The dilute polymer solution's resistance to vortex stretching could inhibit both of these processes. The results in figure 8 show that the average time between the bursts of an individual streak in the drag-reducing solution has the value expected for a water flow at the reduced wall shear. Consequently, these data suggest that the lower than expected spatially averaged bursting rate is the result of the solution inhibiting the formation of streaks.

The suppression of streak formation by the resistance to spanwise vortex stretching is also consistent with the motion pictures. These pictures qualitatively

indicate that the spanwise velocity gradients and the spanwise fluctuation intensities are much less in the drag-reducing solution than they are in an equivalent wall shear Newtonian flow. This observation is based on the fact that the dye appears to be much more uniformly distributed in the spanwise direction (i.e. the dye shows much less tendency to collect into streaks) and the streaks that do form have much less tendency to oscillate in the spanwise direction. Rudd's (1972) laser anemometer measurements of the spanwise fluctuations in a drag-reducing solution are also consistent with these observations.

Since the conclusions reached above are based on a limited range of experiments with one polymer at a single concentration, they must be regarded as somewhat tentative at this time. It is certainly too soon to conclude that in all cases of drag reduction the streak spacing will be affected to the same degree; in fact, Fortuna's (1971) data suggest that there might well be differences due to the polymer molecule. Our experiments are also not extensive enough to rule out the possibility of several types of bursting suppression occurring after the streaks are formed. For example it cannot be determined from the present data whether one or more of the modes of oscillatory growth are preferentially decreased. In short there may be cases where the solution inhibits an oscillatory mode without affecting the streak spacing and there may be cases where both oscillatory growth and streak formation are affected simultaneously and to various degrees. Curiously enough, despite the average results shown in figures 5–7, our motion pictures do show streaks that lift and then after neither oscillating nor bursting return to the wall. Moreover, the general appearance of a drag-reducing wall layer differs enough from a water flow that much more data needs to be analysed before the interactions in a drag-reducing flow can be completely understood. Nevertheless, the importance of the explanation of drag reduction given above should not be minimized. It does rationally explain the present data and it does yield hypotheses to be tested by further experiments.

The visual results of this study also provide a perspective from which some of the more noteworthy models of drag reduction may be reviewed. Virk (1971) has proposed a phenomenological explanation for drag reduction based on an 'elastic sublayer' model. This explanation and many others that are based on interpreting changes in the 'law of the wall' do not seem to hold promise in giving much further insight into the drag-reduction phenomena. This conclusion is based upon several facts. First, the 'law of the wall' does not contain any information about the physical structure of the sublayer. In fact, on the basis of the $U^+ = y^+$ velocity profiles, early investigators reasoned that the sublayer was laminar. This is clearly incorrect and demonstrates the danger of inferring 'details' from an average. Since drag reduction occurs with and apparently because of changes in the structure of the sublayer, it seems almost certain that a thoroughly adequate explanation of the drag-reduction phenomena must be based upon an understanding of these changes in the sublayer structure.

Black (1969) has proposed that the polymers act to stabilize the sublayer breakdown process (i.e. stabilize the bursting process) such that the non-dimensional time between bursts should be increased from $v^*\overline{T}_B/\nu = 116$ for a normal Newtonian flow to $v^*\overline{T}_B/\nu \approx 1400$ for a maximum drag-reducing flow.

Our data indicate that the non-dimensional time between bursts is essentially constant. In addition, Black's analysis does not consider the three dimensionality of the sublayer (i.e. the spanwise velocity variations illustrated by the streaky structure). Since the visual data show that the spanwise velocity distribution is significantly altered in drag-reducing flows, this important characteristic must be considered in any proposed explanation of drag reduction. This criticism applies to all two-dimensional surface renewal models.

On the other hand, Fortuna's (1971) models consider only changes in λ^+ and do not allow for any potential changes in the bursting rate of a streak. The models predict that the streak spacing will become extremely large ($\lambda^+ > 500$) as the maximum drag-reduction limit is approached. The limiting behaviour of these models does not appear reasonable because λ^+ is increasing at a faster than linear rate for the larger values of drag reduction. As an aside it should be pointed out that the streak-spacing measurements of Kline *et al.* (1967) for strongly accelerating flows,

$$K = \frac{\nu}{U_\infty^2}\frac{dU_\infty}{dx} = 3{\cdot}25 \times 10^{-6},$$

yielded $\lambda^+ = 256$ and $\bar{T}_B = 5{\cdot}8$ s/burst. This flow was very nearly relaminarized according to the heat-transfer experiments of Moretti & Kays (1965), which show 'laminar-like' Stanton numbers for $K > 3{\cdot}7 \times 10^{-6}$. The important point here is that for a nearly relaminarized sublayer the streak spacing had increased but not to an extent which appears consistent with the Fortuna models or for that matter with the data of Fortuna & Hanratty (1972) and Eckelman *et al.* (1972).

The findings of this study also show that the proper characteristic length and time scales for drag-reduction characterization are to be found in the viscous sublayer. So far, the wall-shear velocity has been found to correlate much of the drag-reduction data for a given polymer–solvent combination. The failure of the Deborah number of the H parameter of Walsh (1967), which is essentially a concentration-dependent Deborah number, may well be related to the fact that the molecular relaxation time is poorly characterized by the intrinsic viscosity. The data of Paterson & Abernathy (1970) strongly indicate that the molecular relaxation time should be based only on the molecular weight fraction which is effective. In general, this is the highest molecular weight fraction. It also seems likely that the viscosity in axisymmetric strain is the correct property to use with v^* to obtain a non-dimensional 'fluid time'. The possibility still exists of course that the proper fluid time is associated with the oscillatory growth of the bursting process.

In summary, the data show that the flow structure near the wall in a drag-reducing flow is significantly different from a water flow at the reduced wall shear. A rational explanation of how the polymer can accomplish these changes based upon the suppression of vortex stretching during streak formation is offered. Although this conclusion needs to be confirmed through additional experimentation, it is certainly now clear that adequate characterization of drag reduction will be based upon time and length scales associated with the streaky structure in the wall region.

The authors gratefully acknowledge the financial assistance provided to G. L. Donohue through an NDEA Title IV Fellowship and the support of the Office of Engineering Research at Oklahoma State University. Prof. W. B. Brooks, Prof. D. K. McLaughlin and Prof. P. M. Moretti provided many helpful suggestions and criticisms throughout the study.

REFERENCES

BLACK, T. J. 1969 In *Viscous Drag Reduction* (ed. C. S. Wells), pp. 383–407. New York: Plenum.

CLARK, J. A. 1968 *Trans. A.S.M.E., J. Basic Engng*, D **90**, 455.

CLARK, J. A. & MARKLAND, E. 1971 *Proc. A.S.C.E., J. Hydraulics Div.* **97**, 1653.

CORINO, E. R. & BRODKEY, R. S. 1969 *J. Fluid Mech.* **37**, 1.

DONOHUE, G. L. 1972 The effect of a dilute, drag-reducing macromolecular solution on the turbulent bursting process. Ph.D. thesis, Oklahoma State University.

DONOHUE, G. L., MCLAUGHLIN, D. K. & TIEDERMAN, W. G. 1972 *Phys. Fluids* (to be published).

DONOHUE, G. L. & TIEDERMAN, W. G. 1971 The effect of a dilute, drag-reducing macromolecular solution on the viscous sublayer of a turbulent channel flow (16 mm motion picture). Submitted to ASME/ESL Film Library, New York.

ECKELMAN, L. D., FORTUNA, G. & HANRATTY, T. J. 1972 *Nature*, **236**, 94.

FORTUNA, G. 1971 Effect of drag-reducing polymers on flow near a wall. Ph.D. thesis, University of Illinois.

FORTUNA, G. & HANRATTY, T. J. 1972 *J. Fluid Mech.* **53**, 575.

GADD, G. E. 1965 *Nature*, **206**, 463.

GUPTA, A. K., LAUFER, J. & KAPLAN, R. E. 1971 *J. Fluid Mech.* **50**, 493.

HALLEEN, R. M. & JOHNSTON, J. P. 1967 *Stanford University Rep.* MD-18.

HUSSAIN, A. K. M. F. & REYNOLDS, W. C. 1970 *Stanford University Rep.* FM-6.

KIM, H. T., KLINE, S. J. & REYNOLDS, W. C. 1971 *J. Fluid Mech.* **50**, 133.

KLINE, S. J., REYNOLDS, W. C., SCHRAUB, F. A. & RUNSTADLER, P. W. 1967 *J. Fluid Mech.* **30**, 741.

LAUFER, J. & BADRI NARAYANAN, M. A. 1971 *Phys. Fluids*, **14**, 182.

LUMLEY, J. L. 1969 In *Annual Reviews of Fluid Mechanics*, vol. 1 (ed. W. R. Sears), pp. 367–384. Annual Reviews Inc.

MERRILL, E. W., SMITH, K. A., SHIN, H. & MICKLEY, H. S. 1966 *Trans. Soc. Rheology*, **10**, 335.

MORETTI, P. M. & KAYS, W. M. 1965 *Int. J. Heat & Mass Transfer*, **8**, 1187.

PATERSON, R. W. & ABERNATHY, F. H. 1970 *J. Fluid Mech.* **43**, 689.

RAO, K. N., NARASIMHA, R. & BADRI NARAYANAN, M. A. 1971 *J. Fluid Mech.* **48**, 339.

RUDD, M. J. 1972 *J. Fluid Mech.* **51**, 673.

RUNSTADLER, P. W., KLINE, S. J. & REYNOLDS, W. C. 1963 *Stanford University Rep.* MD-8.

VIRK, P. S. 1971 *J. Fluid Mech.* **45**, 417.

WALLACE, J. M., ECKELMANN, H. & BRODKEY, R. S. 1972 *J. Fluid Mech.* **54**, 39.

WALSH, M. 1967 On the turbulent flow of dilute polymer solutions. Ph.D. thesis, California Institute of Technology.

WELLS, C. S. & SPANGLER, J. G. 1967 *Phys. Fluids*, **10**, 1890.

WHITSITT, N. F., HARRINGTON, L. J. & CRAWFORD, H. R. 1969 In *Viscous Drag Reduction* (ed. C. S. Wells), pp. 265–280. New York: Plenum.